
MiR-146a down-regulates inflammatory response by targeting TLR3 and TRAF6 in Coxsackievirus B infection

YANRU FEI,¹ ANITA CHAULAGAIN,¹ TIANYING WANG,¹ YANG CHEN,¹ JINCHANG LIU,¹ MING YI,¹ YING WANG,¹ YIKE HUANG,² LEXUN LIN,¹ SIJIA CHEN,¹ WEIZHEN XU,¹ LEI TONG,¹ XIAOYU WU,³ DECHAO ZHAO,³ FENGMING ZHANG,¹ WENRAN ZHAO,² and ZHAOHUA ZHONG¹

¹Department of Microbiology, ²Department of Cell Biology, Harbin Medical University, Harbin 150081, China

³Department of Cardiology, The First Hospital of Harbin Medical University, Harbin 150001, China

ABSTRACT

Coxsackievirus B (CVB) is the major cause of human myocarditis and dilated cardiomyopathy. Toll-like receptor 3 (TLR3) is an intracellular sensor to detect pathogen's dsRNA. TLR3, along with TRAF6, triggers an inflammatory response through NF- κ B signaling pathway. In the cells infected with CVB type 3 (CVB3), the abundance of miR-146a was significantly increased. The role of miR-146a in CVB infection is unclear. In this study, TLR3 and TRAF6 were identified as the targets of miR-146a. The elevated miR-146a inhibited NF- κ B translocation and subsequently down-regulated proinflammatory cytokine expression in the CVB3-infected cells. Therefore, the NF- κ B pathway can be doubly blocked by miR-146a through targeting of TLR3 and TRAF6. MiR-146a may be a negative regulator on inflammatory response and an intrinsic protective factor in CVB infection.

Keywords: Coxsackievirus B; miR-146a; TLR3; TRAF6; NF- κ B

INTRODUCTION

Coxsackievirus group B (CVB) belongs to the *Enterovirus* genus of the Picornaviridae family (Kim et al. 2008; Ye et al. 2013; Garmaroudi et al. 2015) and is the major cause of human myocarditis and dilated cardiomyopathy (Tong et al. 2011; Gui et al. 2012; Ye et al. 2013; Garmaroudi et al. 2015). Aggravated inflammatory response of the CVB-infected cells damages myocardial tissues and leads to heart failure (Verma et al. 2010; Yin et al. 2014; Garmaroudi et al. 2015). CVB also has been reported to cause a wide range of other infections such as meningitis, pancreatitis, and meningoencephalitis (Ye et al. 2013; Yin et al. 2014; Sesti-Costa et al. 2017).

Toll-like receptors (TLRs) are cellular sensors that recognize the danger signals such as pathogen-associated molecular pattern (PAMP) and danger-associated molecular pattern (DAMP) (Janssens and Beyaert 2003; Taganov et al. 2006). TLR3, TLR7, TLR8, and TLR9 locate in the endosomal membrane and exclusively detect intracellular danger signals (Kawai and Akira 2007; Blasius and Beutler 2010). The CVB genome is a single-stranded positive sense RNA (+ssRNA) (Wang et al. 2014; Sesti-Costa et al. 2017).

During its replication, a double-stranded RNA (dsRNA) intermediate is generated so as to produce progeny copies of the +ssRNA genome (Marchant et al. 2008). Viral dsRNA is a typical PAMP molecule and can be recognized by TLR3 (Matsumoto et al. 2011; Oshiumi et al. 2011). TLR3 transfers the risk signal to nuclear factor-kappa B (NF- κ B) through the activations of TRIF (TIR-domain-containing adapter-inducing interferon- β), TRAF6 (tumor necrosis factor receptor-associated factor 6), and IRAK1 (Interleukin-1 receptor-associated kinase 1) (Kawai and Akira 2007, 2011; Fukushima et al. 2018). Activated NF- κ B leads to the translocation of its p50 and p65 subunits from cytoplasm to the nucleus and drives the expression of proinflammatory cytokines (Janssens and Beyaert 2003; Kawai and Akira 2007, 2011). Previous studies have shown that in CVB-related myocarditis, NF- κ B is activated to increase the expression of proinflammatory cytokines, enzymes, and adhesion molecules (O'Neill et al. 2011; Garmaroudi et al. 2015). Disseminating cytokines are found in abundant amounts in viral myocarditis patients and negatively affect heart tissues (Garmaroudi et al. 2015).

Corresponding authors: zhongzh@hrbmu.edu.cn, zhongwr@ems.hrbmu.edu.cn

Article is online at <http://www.majournal.org/cgi/doi/10.1261/rna.071985.119>.

© 2020 Fei et al. This article is distributed exclusively by the RNA Society for the first 12 months after the full-issue publication date (see <http://majournal.cshlp.org/site/misc/terms.xhtml>). After 12 months, it is available under a Creative Commons License (Attribution-NonCommercial 4.0 International), as described at <http://creativecommons.org/licenses/by-nc/4.0/>.

MicroRNAs (miRNAs) are a cluster of short, single-stranded noncoding RNAs, which can posttranscriptionally regulate the gene expression by binding to the 3' untranslated region (3'UTR) of the target mRNAs (Ghose et al. 2011; Wang et al. 2012; Li et al. 2016; Min et al. 2017; Trobaugh and Klimstra 2017). MiRNAs can also bind to the 5'UTR and coding regions of the targets (Wu et al. 2015). It has been widely accepted that miRNAs play an important role in innate immunity, cell development, apoptosis, and signal transduction (Labbaye and Testa 2012; Wu et al. 2015). Recent studies reveal that miRNAs are actively involved in the regulation of the TLR-signaling pathway. TLR4 and TLR2, two receptors for recognizing extracellular pathogens, are the targets of let-7, miR-233, miR-26a, and miR-146a (He et al. 2014). TLR3 is the target of miR-233 and miR-26a (Johnnidis et al. 2008; He et al. 2014; Jiang et al. 2014). Signaling proteins can also be targeted by miRNAs. IRAK1/2/4 and TRAF6 are the targets of miR-146a (Taganov et al. 2006). FADD, IKK β / ϵ , TAB2, and RIPK1 are the targets of miR-155 (Tili et al. 2007; Ceppi et al. 2009; He et al. 2014).

In this study, we found that miR-146a levels were significantly elevated in the CVB3-infected cells. We further identified TLR3, along with TRAF6, as the targets of miR-146a. Therefore, TLR3 and NF- κ B signaling pathways could be doubly blocked by miR-146a through targeting TLR3 and TRAF6 during CVB infection.

RESULTS

MiR-146a expression is elevated in the CVB3-infected cells

We first isolated cardiac fibroblasts from suckling Balb/c mice and obtained the miRNA expression profile in the primary cells with CVB3 infection (MOI = 5). Microarray detection (Supplemental Dataset 1 and 2) showed that most miRNAs were down-regulated, whereas only a few miRNAs were up-regulated compared with the noninfected control cells. MiR-146a expression remained elevated at 24 and 48 h postinfection (p.i.) (Fig. 1A,B).

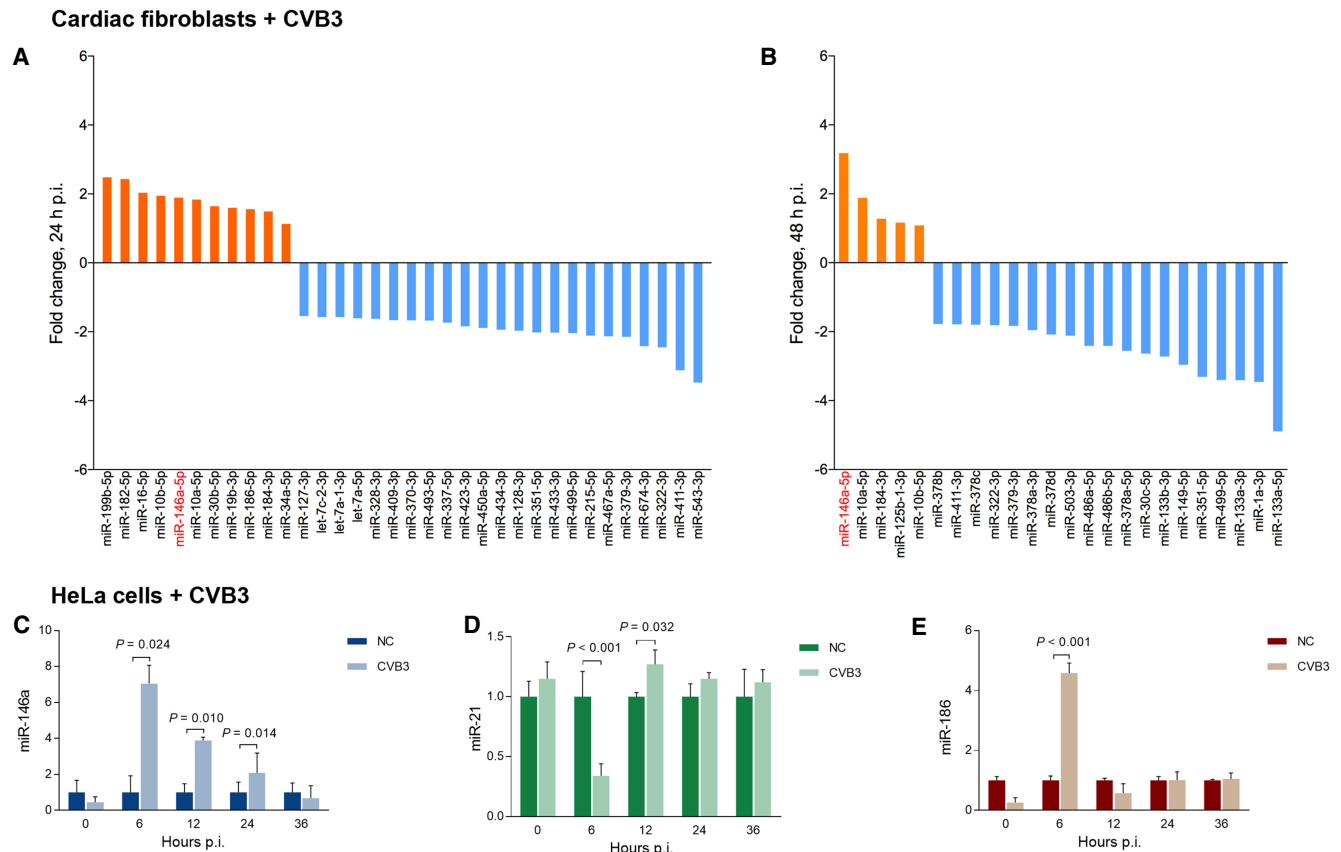


FIGURE 1. MiR-146a abundance in the CVB3-infected cells. (A,B) Primary cardiac fibroblasts isolated from Balb/c mouse were infected with CVB3 (MOI = 5). Total RNA was collected at 24 and 48 h p.i. and subjected to miRNA array detection. (C–E) HeLa cells were infected with CVB3 (MOI = 1). The abundances of miR-146a, miR-21, and miR-186 at 0, 6, 12, 24, and 36 h p.i. were detected by RT-qPCR with the $\Delta\Delta C_T$ method. The abundance of miRNAs was normalized by U6 (miRNAs). Error bars represent standard deviation (SD), *n* = 4.

To validate the microarray observation, the abundance of miR-146a in the CVB3-infected HeLa cells (MOI = 1) was detected by RT-qPCR. Consistently, the level of miR-146a was significantly elevated from 6 to 24 h p.i. in the infected cells (Fig. 1C). As controls, the abundance of miR-21 and miR-186 changed temporarily at 6 h p.i. but later remained the same as in the normal control (NC) cells (Fig. 1D,E). The miR-146a level dropped in the infected HeLa cells at 36 h p.i. because only a few cells survived after CVB3 infection at that time point. Cardiac fibroblasts are very tolerant of CVB3; thus, a prolonged elevated expression of miR-146a was observed.

TLR3 and TRAF6 are the targets of miR-146a

To identify the role of miR-146a in CVB infection, the targets of miR-146a were screened by TargetScan 7.1 and RNAhybrid 2.2. As shown in Figure 2A,B, both tools predicted TLR3 and TRAF6 as its potential targets. Two target sites in TLR3 mRNA (nt1985–nt1992 and nt2885–nt2891), and three target sites in TRAF6 mRNA (nt473–nt480, nt538–nt545, and nt1272–nt1279) were identified.

To validate the prediction, HeLa cells were transfected with synthesized miR-146a mimics or anti-miR-146a oligonucleotide (AMO-146a). At 24 h posttransfection, the

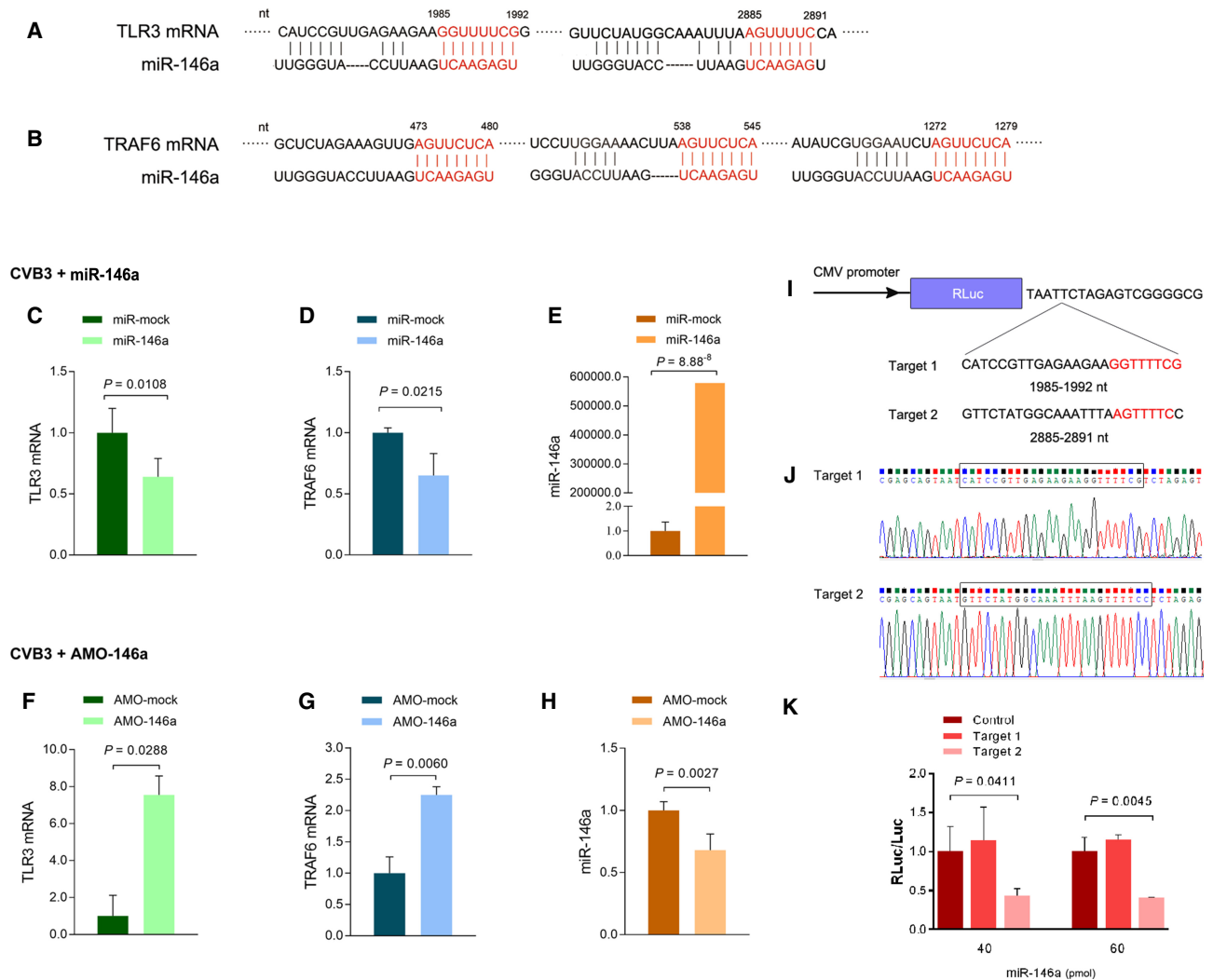


FIGURE 2. TLR3 and TRAF6 are the targets of miR-146a. (A,B) There are two sites in TLR3 mRNA and three sites in TRAF6 mRNA that perfectly match to the seed sequence of miR-146a. (C–E) HeLa cells were transfected with miR-146a mimics and infected with CVB3 (MOI = 1) 24 h posttransfection. The mRNA abundances of TLR3 and TRAF6 were quantified by RT-qPCR with the $\Delta\Delta C_T$ method. (F–H) HeLa cells were transfected with AMO-146a and infected with CVB3 (MOI = 1) 24 h posttransfection. The mRNA abundances of TLR3 and TRAF6 were quantified by RT-qPCR with the $\Delta\Delta C_T$ method. The mRNA abundances of TLR3 and TRAF6 were normalized by GAPDH mRNA, whereas miR-146a was normalized by U6 snRNA. Error bars represent SD, $n = 4$. (I–K) Two putative targets of TLR3 (1985–1992 nt and 2885–2891 nt) were inserted separately into the 3'UTR sequence of *Renilla* luciferase (RLuc) gene in plasmid pGL4.75. The modified pGL4.75 was transfected with *Firefly* luciferase (Luc)-expressing plasmid pGL4.17 and 40 or 60 pmol of miR-146a simultaneously to HeLa cells. Luciferase expression in these cells was detected at 24 h posttransfection. The level of RLuc in each well was normalized by Luc. Error bars represent SD, $n = 3$.

RNAs and proteins were extracted for RT-qPCR and western blotting. MiR-146a mimics effectively decreased the mRNA abundance of TLR3 and TRAF6 (Fig. 2C,D). As a control, TLR7 mRNA abundance was not affected by miR-146a mimics (Supplemental Fig. S1). Consistently, in the cells with AMO-146a, miR-146a knockdown significantly increased the level of TLR3 mRNA (Fig. 2F) and TRAF6 mRNA (Fig. 2G), whereas the level of TLR7 mRNA was not affected by AMO-146a (Supplemental Fig. S1). To further verify the targets, a luciferase reporter system was constructed (Fig. 2I,J). As shown in Figure 2K, the sequence of nt2885–nt2891 of TLR3 mRNA could be effectively targeted by miR-146a.

To examine the protein expression of TLR3 and TRAF6, HeLa cells were transfected with miR-146a mimic or AMO-

146a as described above. The cells were stimulated with lipopolysaccharide (LPS) 6 h before harvesting the cell lysate. Western blotting demonstrated that the protein levels of TLR3 and TRAF6 were also decreased by miR-146a (Fig. 3A,B) and increased by AMO-146a (Fig. 3C,D). The changes became more prominent in the cells with LPS stimulation. Our evidence indicates that the expression of TLR3 and TRAF6 can be regulated by miR-146a.

MiR-146a suppresses the TLR3-NF-κB pathway

TLR3 senses intracellular risk signals such as pathogen’s dsRNA in the endosomes and triggers an inflammatory response through the downstream players including TRAF6 and NF-κB. To verify the impact of miR-146a on TLR3 and

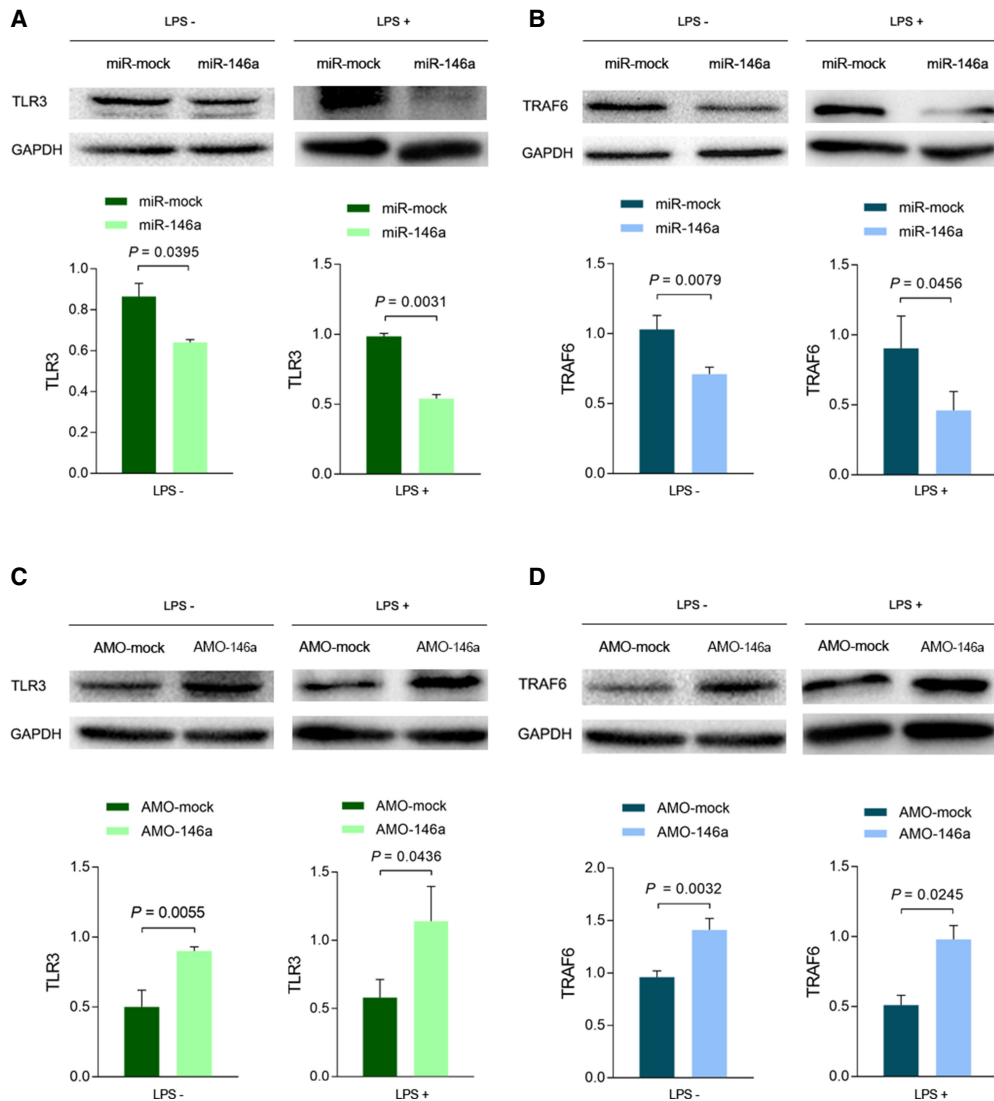


FIGURE 3. Validation of miR-146a targeting to TLR3 and TRAF6. HeLa cells were transfected with miR-146a mimics, AMO-146a, and scramble RNAs, respectively. A group of the transfected cells were treated with LPS at 24 h posttransfection. Total protein was extracted at 24 h posttransfection or 6 h after the LPS treatment. The protein levels of TLR3 (A,C) and TRAF6 (B,D) were detected by western blotting. GAPDH was used as a loading control. Error bars represent the SD, n = 3.

TRAF6, HeLa cells were transfected with miR-146a mimics or AMO-146a and stimulated with LPS. The translocation of the NF- κ B p65 subunit was detected to determine whether the signaling pathway is activated. In the HeLa cells transfected with miR-146a mimics, the nuclear portion of p65 was significantly decreased, whereas the cytoplasmic portion of p65 was increased (Fig. 4A,B). On the contrary, the nuclear portion of p65 was increased and the cytoplasmic portion of p65 was decreased in the cells with AMO-146a (Fig. 4C,D). In both situations, there was no significant difference found in the total amount of p65. A similar result was also observed in the cells without LPS treatment (Supplemental Fig. S2). A luciferase reporter assay was used to further verify the effect of miR-146a on NF- κ B.

Similarly, miR-146a could suppress NF- κ B activation, and AMO-146a could reverse the suppression in a dose-dependent manner (Fig. 4E,F). The expression of proinflammatory cytokines IL-6 and TNF- α is typically controlled by NF- κ B. RT-qPCR showed the mRNA expression of IL-6, and TNF- α was significantly decreased in the cells with miR-146a but increased in the cells with AMO-146a (Fig. 4G,H). Consistently, ELISA showed that the IL-6 and TNF- α significantly decreased in the culture medium of the cells with miR-146a, whereas they increased when the cells were treated with AMO-146a (Fig. 4G,H). The data consistently support that miR-146a down-regulates NF- κ B and an inflammatory response by targeting TLR3 and TRAF6.

TLR3 and TRAF6 are down-regulated by miR-146a in the CVB3-infected cells

To evaluate the impact of miR-146a on CVB3 infection, the expression of TLR3 and TRAF6 in the HeLa cells with CVB3 and AMO-146a, separately or together, were detected by western blotting. TLR3 expressed increasingly in the cells treated with CVB3 alone. When miR-146a was knocked down by AMO-146a, TLR3 expression was further elevated (Fig. 5A,B), suggesting that TLR3 expression was negatively regulated by miR-146a in the infected cells. Unlike TLR3, TRAF6 expression was decreased in the cells with CVB3 alone, but significantly increased in the infected cells with AMO-146a (Fig. 5A,C). It is interesting that the highest levels of TLR3 and TRAF6 were observed in the cells treated with AMO-146a alone, probably because of the antagonist effect of AMO-146a against the baseline expression of miR-146a.

Enterovirus 71 (EV71), a member of the Picornaviridae family, is a close sibling of CVB. EV71 is one of the major causes of hand, foot, and mouth disease (HFMD) and encephalitis in children (Tili et al. 2007; Ho et al. 2015; Zheng et al. 2017). We found that the expression of TLR3 and TRAF6 to the treatment of AMO-146a shared the same pattern in the EV71- and CVB3-infected cells (Fig. 5D–F), suggesting that miR-146a plays a similar role in EV71 infection.

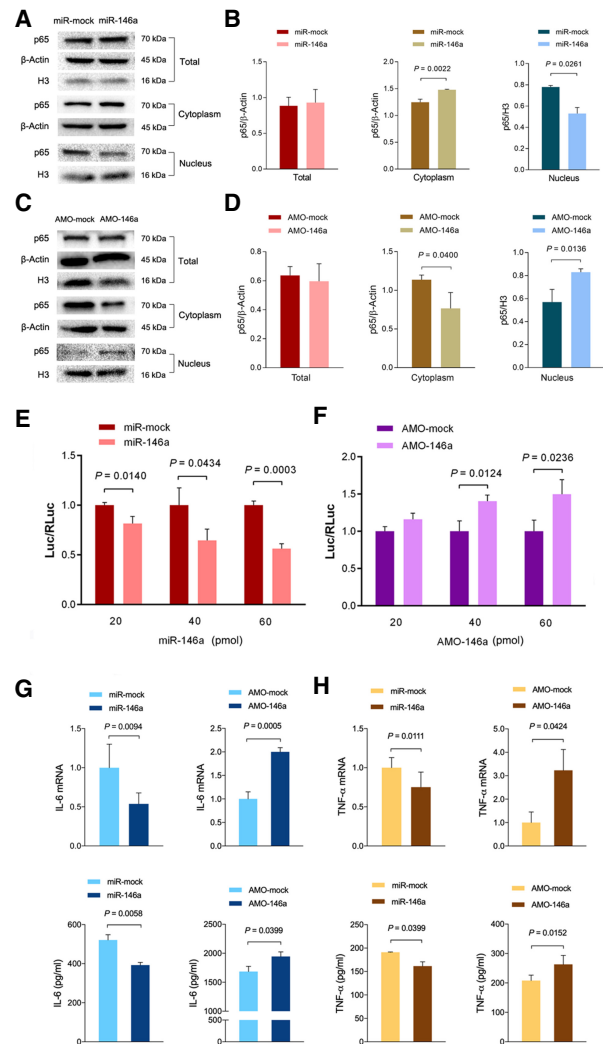


FIGURE 4. Effect of miR-146a on NF- κ B translocation. HeLa cells were first treated with miR-146a mimics, AMO-146a, and scramble RNAs, respectively. The cells were treated with LPS at 18 h and harvested 24 h after the transfection. (A–D) Total, cytoplasmic, and nuclear portions of the p65 subunit of NF- κ B were analyzed by western blotting. Total and cytoplasmic proteins were normalized using β -actin, whereas histidine H3 was used to normalize nuclear protein. (E,F) Detection of NF- κ B activation with luciferase reporter assay. pNF- κ B-Luc (Stratagene) is a plasmid in which *Firefly* luciferase (Luc) expression is modulated by an NF- κ B response element. NF- κ B activation can be measured by the level of Luc expression. HeLa cells were transfected with pNF- κ B-Luc, pRL-TK, and various RNAs. The expression of Luc and RLuc in these cells was detected with dual luciferase reagents at 24 h posttransfection. (G,H) The mRNA and protein of IL-6 and TNF- α were detected with RT-qPCR and western blotting, respectively. Error bars represent SD, $n = 3$.

The TLR3-NF- κ B pathway is inhibited by miR-146a in the CVB3-infected cells

HeLa cells were treated with CVB3 and AMO-146a, separately or together. The level of the NF- κ B p65 subunit in the total, cytoplasmic, and nuclear fractions of protein extractions was detected by western blotting. Total p65 did

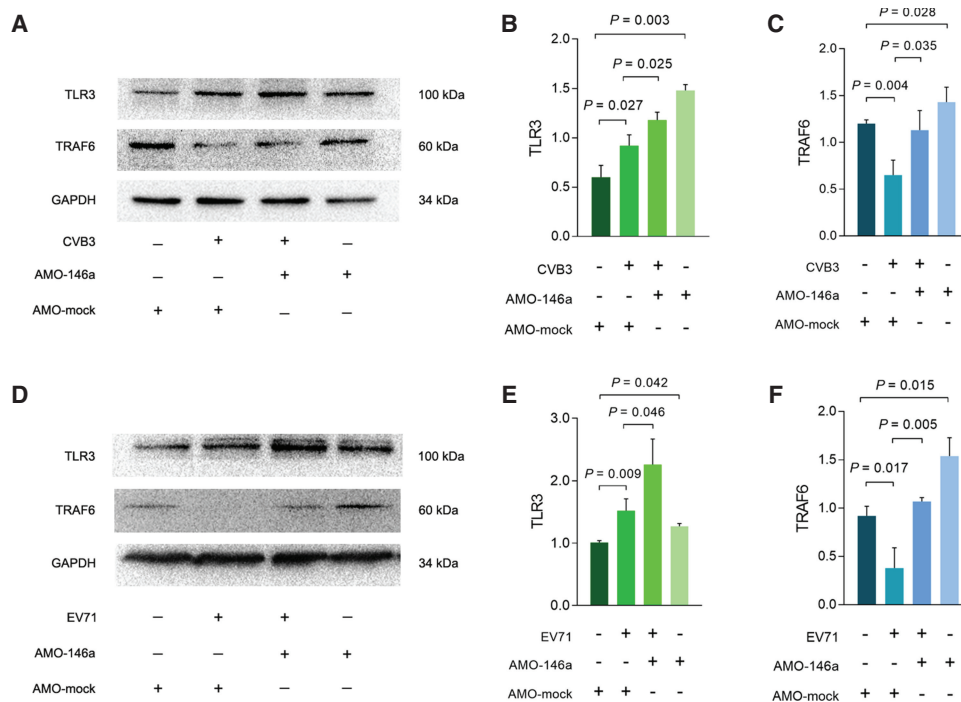


FIGURE 5. The expression of TLR3 and TRAF6 in the CVB3- and EV71-infected cells. HeLa cells were treated with AMO-146a or scramble RNA. CVB3 and EV71 were infected at 12 h posttransfection, respectively. TLR3 and TRAF6 were detected with western blotting in the cells with CVB3 infection (A–C) and EV71 infection (D–F). TRAF6 and TLR3 were normalized by GAPDH. Error bars represent SD, $n = 3$.

not change apparently in the cells with various treatments, but the nuclear p65 fraction increased significantly in the CVB3-infected cells. When the cells were treated with AMO-146a and CVB3, the nuclear p65 was further increased significantly compared to that in the cells with CVB3 alone (Fig. 6A), whereas the cytoplasmic p65 was decreased in the cells with CVB3 infection and AMO-146a (Fig. 6A). Approximately 30% of p65 was blocked from nuclear translocation by miR-146a in the CVB3-infected cells.

Consistently, RT-qPCR showed that mRNA expression for proinflammatory cytokines, IL-6 and TNF- α , was significantly elevated in the CVB3-infected cells. A further increase in these mRNAs was observed in the cells with CVB3 and AMO-146a (Fig. 6B,C). The data suggest that the elevated miR-146a plays a suppressive role in the TLR3-NF- κ B pathway and, subsequently, would partially block the innate antiviral immunity against CVB.

DISCUSSION

TLR3 is an intracellular sensor that recognizes a pathogen’s dsRNA and transfers the risk signal to the nucleus through TRAF6 and the NF- κ B pathway (Oshiumi et al. 2011; Zhang et al. 2013; Sanghavi and Reinhart 2014). Enteroviruses replicate solely in the cytoplasm and need a dsRNA intermediate to generate its progeny +ssRNA genome; thus, enterovirus replication can be sensed by TLR3 (Chen et al. 2018). In addition, the enteroviral +ssRNA genome

can also be sensed by TLR3 through its incomplete stem structures (Tatematsu et al. 2013). TLR3 activation leads to innate immune responses against the invaded pathogens, including triggering inflammation by NF- κ B signaling cascade and inducing type I IFN expression by activating IRF3 and IRF7 (Pérez De Diego et al. 2014). However, in the present study, our evidence indicates that miR-146a could doubly block the NF- κ B pathway by targeting TLR3 and its downstream player TRAF6. Based on our findings and accumulated data, we hypothesize that miR-146a is a negative regulator on the inflammation response in CVB infection. With the help of miR-146a, the host can balance inflammatory response at an adequate level so as to kill pathogens but not badly hurt the host itself. CVB may benefit from miR-146a’s negative regulation to evade the host innate immune response.

We repeatedly observed elevated miR-146a expression in CVB infection. The cells and tissues we had detected included mouse myocardial tissues, myocytes, cardiac fibroblasts, and HeLa cells (Fig. 1 shows data of cardiac fibroblasts and HeLa cells). Interestingly, only a few of miRNAs were up-regulated in the CVB-infected cells and tissues. We have previously evaluated the role of miR-10a and found that miR-10a*, the star strand of miR-10a, specifically promotes CVB replication, thus is a host factor for the myocardial tropism of CVB (Tong et al. 2013). However, the role of miR-146a in CVB infection remains elusive.

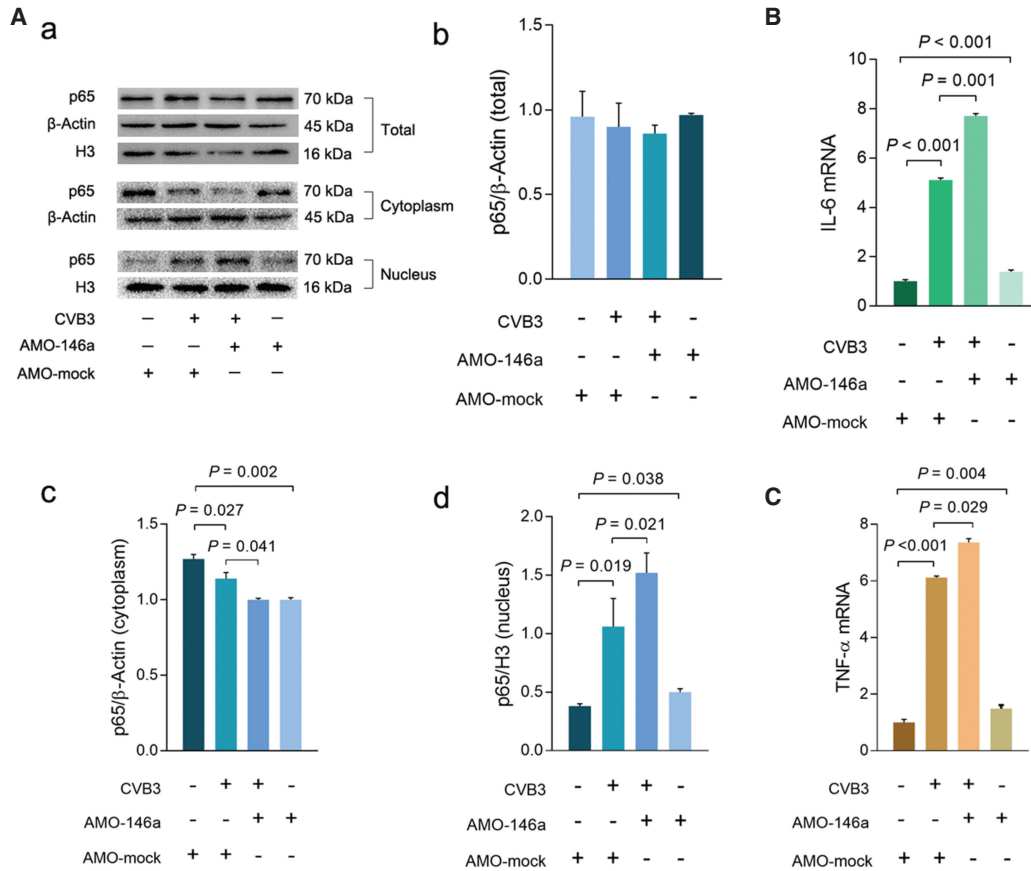


FIGURE 6. The TLR3-NF- κ B pathway is inhibited by miR-146a in CVB3 infection. HeLa cells were treated with AMO-146a and scramble RNA, respectively. These cells were infected with CVB3 12 h posttransfection. (A) Total, cytoplasmic, and nuclear proteins were extracted 24 h p.i. The p65 subunit of NF- κ B was detected with western blotting. The cytoplasmic fraction was normalized by β -actin, and the nuclear fraction was normalized by histidine H3. (B,C) The mRNA abundance of IL-6 and TNF- α were quantified by RT-qPCR. Error bars represent SD, $n = 3$.

Upon bioinformatical analysis, two sequences in TLR3 mRNA were identified as the targets of miR-146a. Previously, TRAF6 has been identified as a target of miR-146a (Taganov et al. 2006; Ghose et al. 2011; He et al. 2014; Kamali et al. 2016; Lee et al. 2016). Our experiments confirmed that miR-146a mimics decreased the expression of TLR3 and TRAF6, whereas AMO-146a could reverse miR-146a's suppression on TLR3 and TRAF6, both in non-infected and CVB3-infected cells (Figs. 2, 3, and 5A). With a luciferase reporter, the sequence of nt2885–nt2891 in TLR3 mRNA was verified as the target of miR-146a (Fig. 2K). A similar effect of miR-146a was also observed in the cells infected with EV71 (Fig. 5D). Our data confirmed that TLR3 and TRAF6 were modulated by miR-146a.

Several innate immune signaling proteins such as TRAF6 and IRAK1 have been identified as the targets of miR-146a (Taganov et al. 2006; Ghose et al. 2011; He et al. 2014; Kamali et al. 2016; Lee et al. 2016). Therefore, miR-146a is considered as an innate immune inhibitor. Inflammation is a major event in the myocardial infection caused by CVB. Proinflammatory cytokines IL-6 and TNF- α are up-regulated in the CVB-infected cells

(Gui et al. 2012). We observed a similar result in the CVB3-infected cells (Fig. 6). However, treatment with AMO-146a in the CVB3-infected cells caused a 15%–20% increase in the mRNAs of TNF- α and IL-6 compared with that in the cells with CVB3 alone (Fig. 6), suggesting that miR-146a plays a suppressor role in the inflammatory response to CVB infection.

Given the catastrophic consequence of inflammatory response in the myocarditis caused by CVB, up-regulated miR-146a expression may be a cellular physiological response. Indeed, Taganov et al. (2006) revealed that miR-146a expression is NF- κ B-dependent. There are three NF- κ B-binding sites in the upstream sequence of miR-146a genomic locus on chromosome 5. In this study, our data demonstrate that NF- κ B was activated in the cells with CVB infection (Fig. 6). Therefore, we hypothesize that CVB3 first activates the NF- κ B pathway and then triggers an inflammatory response. The activated NF- κ B translocates to the nucleus and binds to the genomic locus of miR-146a to initiate the transcription of miR-146a. Conversely, miR-146a suppresses the NF- κ B pathway by down-regulating TLR3 and TRAF6 and alleviates the

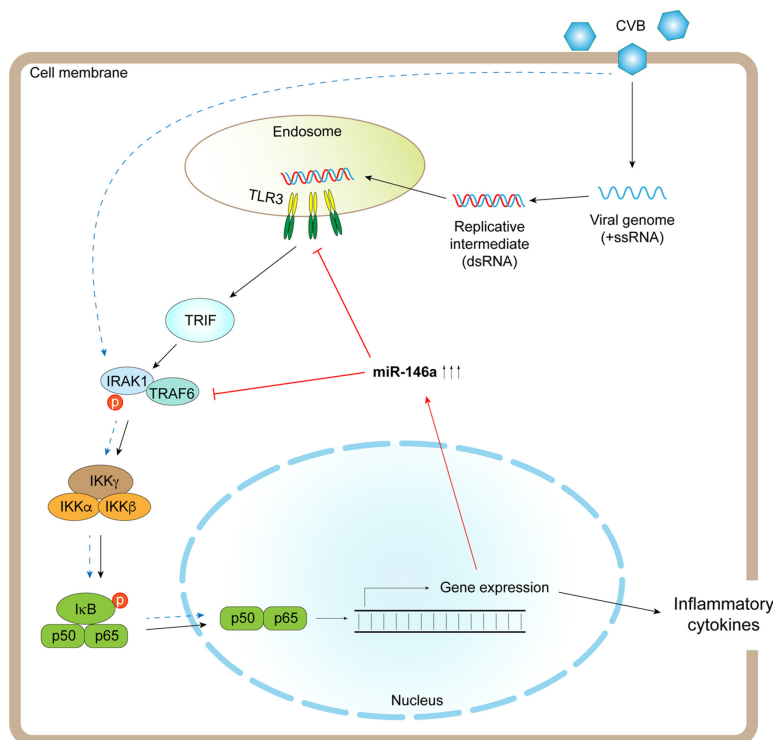


FIGURE 7. The putative role of miR-146a in CVB infection. CVB3 triggers an inflammatory response by activating NF-κB through multiple inductions (dashed lines). The activated NF-κB translocates to the nucleus and binds to the genomic locus of miR-146a in chromosome 5 to initiate the transcription of the downstream RNA including primary miR-146a. After a mature process, miR-146a conversely suppresses the NF-κB pathway by doubly blocking TLR3 and TRAF6. Through the negative feedback by miR-146a, the inflammation caused by CVB can be precisely controlled to an adequate level so that the viruses can be eliminated but the tissue is not overinjured.

inflammatory response. Through the regulatory loop, the inflammation can be precisely controlled to a level adequate to eliminate the invading viruses without badly hurting the host. A putative mechanism is summarized in Figure 7.

In this study, endotoxin LPS was used to stimulate the cells. LPS is not a canonical ligand of TLR3. We chose LPS rather than poly(I:C) because poly(I:C) cannot induce miR-146a expression (data not shown). In the LPS-treated cells, TLR3 expression was up-regulated (Fig. 3). A similar observation has been reported (Taganov et al. 2006). A limitation in this study is that we did not test the effect of miR-146a on CVB infection in vivo. We found that miR-146a could somehow affect the virus replication (Supplemental Fig. S3). It is hard to interpret that the outcome of animal experiments is caused by blocking the NF-κB pathway or by restricting virus replication.

Taken together, we identified TLR3, along with TRAF6, as the target of miR-146a. TLR3-NF-κB pathway can be doubly suppressed by miR-146a. On the other hand, miR-146a decreases the proinflammatory cytokine expression and may protect the infected one from severe inflammation injury.

MATERIALS AND METHODS

Cells, viruses, and nucleotides

HeLa cells were maintained in Dulbecco Modified Eagle Medium (DMEM) (Hyclone) supplemented with 10% fetal bovine serum (FBS) (Biological Industries) at 37°C with 5% CO₂. The Woodruff strain of CVB type 3 (CVB3) and the BrCr strain of EV71 were passaged in HeLa cells. About 1 multiplicity of infection (MOI) of CVB3 or 10 MOI of EV71 was used to infect HeLa cells for 24 h and the supernatant was stocked at -80°C for further use. Nucleotides, including miR-146a, miR-21, miR-186, miR-mock, AMO-146a (anti-miR-146a oligonucleotide, 5'-AACCCAUGGA AUUCAGUUCUCA-3'), and AMO-mock (5'-CAGUACUUUUGUGUAGUACAA-3'), were synthesized by GenePharma.

MiRNA microarray analysis

Primary cardiac fibroblasts were isolated from suckling Balb/c mice with the digestion of trypsin and collagenase. The cells were infected with CVB3 (MOI = 5) and harvested for miRNA extraction at 24 and 48 h p.i. when ~70%–80% of cells showed cytopathic effects. The miRNAs in the CVB3-infected and uninfected cardiac fibroblasts were isolated with miRNeasy mini kit (QIAGEN). The purified miRNAs were labeled with miRCURY Hy3/Hy5 Power labeling kit (Exiqon) and hybridized with miRCURY LNA Array (Exiqon). The microarray was detected with a GenePix 4000 scanner (Molecular Devices) and the miRNAs with intensities of ≥30 were collected for miRNA profiling analysis.

MiRNA target prediction and verification

RNAhybrid 2.2 (bibiserv.techfak.uni-bielefeld.de/rnahybrid) and TargetScan 7.1 (www.targetscan.org/vert-71) were used for predicting the targets of miRNA. Complementary base sequences with minimum free energy (mfe) were chosen to select the potential binding sites. To verify the predicted targets, the putative target sequences were inserted into the 3'UTR region of *Renilla* luciferase (RLuc) gene in plasmid pGL4.75 (Promega) by overlapping PCR. The modified pGL4.75 was transfected with pGL4.17, a *Firefly* luciferase (Luc)-expressing plasmid (Promega), and 40–60 pmol of miR-146a to HeLa cells. The expression of luciferases was detected at 24 h posttransfection with Dual-Luc reporter reagents (Promega). The RLuc level was normalized with Luc to minimize transfection variation.

RNA transfection

The transfection of miRNAs or AMO-miRNAs was carried out as described previously (Wang et al. 2012). Briefly, HeLa cells were

cultured in DMEM with 10% FBS in six- to 12-well plates and maintained at 37°C with 5% CO₂. After 18–24 h, the media was replaced with serum-free media. Lipofectamine 2000 (Invitrogen) and 1–2 µg of miRNAs or AMO-miRNAs were diluted in serum-free media at room temperature for 20 min and then added to the plate wells. The transfected cells were maintained for 24–36 h at 37°C with 5% CO₂ for further study.

Quantitative real-time polymerase chain reaction (RT-qPCR)

Total RNA was extracted from the treated HeLa cells using TRIzol reagent (Invitrogen). About 1 µg of RNA was subjected to reverse transcription, and 1 µL of the amplified cDNA was mixed with SYBR Premix Ex Taq II (TaKaRa) and sense/antisense primers to a final volume of 25 µL. The RT-qPCR was performed with a CFX96 amplifier (Bio-Rad) as described previously (Wu et al. 2009). The 2^{-ΔΔCt} method (Livak and Schmittgen 2001) was used to calculate the expression of miRNAs and mRNAs. GAPDH mRNA was used as an internal reference. The GAPDH primers were GCACCGTCACGGCTGAGAAC (sense) and TGGTGAAGACGCCAGTGGA (antisense).

Enzyme-linked immunosorbent assay (ELISA)

Cell supernatant was collected and IL-6 and TNF-α expression were determined by using ELISA kits following the manufacturer's instructions (4A Biotech).

Western blot

Total protein was extracted using Pierce RIPA buffer (Thermo Scientific) mixed with phenyl methane sulfonyl fluoride (PMSF). Cytoplasmic and nuclear proteins were isolated by a nuclear and cytoplasmic protein extraction kit (Beyotime) according to the user's manual. Extracted proteins were separated by sodium dodecyl sulfate-polyacrylamide gel electrophoresis (SDS-PAGE) and transferred to a PVDF film (Millipore). The film was incubated with the primary antibody overnight at 4°C. After a standard washing, the film was incubated with horseradish peroxidase (HRP)-labeled secondary antibody for 1 h at room temperature. The blots were imaged by CCD camera FluorChem M (ProteinSimple). The antibodies against TRAF6, TLR3, p65, GAPDH, and H3 were purchased from Proteintech. The antibody against β-actin was purchased from Santa Cruz Biotechnology.

Statistical analysis

Data is presented as mean ± standard deviation (SD). A Student's t-test was performed by Prism 7 (GraphPad Software). All the experiments were repeated at least three times.

SUPPLEMENTAL MATERIAL

Supplemental material is available for this article.

ACKNOWLEDGMENTS

This work was supported by grants of the National Natural Science Foundation of China (81571999 and 81871652 to Z.Z., 81672007 to W.Z., 81772188 to Y.W., and 81570340 to D.Z.). A.C. was supported by the China Scholarship Council (CSC) (2016524006) and the Government of Nepal, Ministry of Education (MOE scholarship no. 8286). Y.F. was supported by Heilongjiang Province Graduate Innovation Research grant (YJSCX2017-9HYD) and T.W. was supported by University Nursing Program for Young Scholars with Creative Talents in Heilongjiang Province grant (UNPYSCT-2016044). S.C. was supported by Health Commission of Heilongjiang Province grant 2014-409. We wish to thank the Heilongjiang Provincial Key Laboratory of Pathogens and Immunity and Northern Translational Medicine Research Centre of Harbin Medical University for their technical support.

Received May 20, 2019; accepted October 28, 2019.

REFERENCES

- Blasius AL, Beutler B. 2010. Intracellular Toll-like receptors. *Immunity* **32**: 305–315. doi:10.1016/j.immuni.2010.03.012
- Ceppi M, Pereira PM, Dunand-Sauthier I, Barras E, Reith W, Santos MA, Pierre P. 2009. MicroRNA-155 modulates the interleukin-1 signaling pathway in activated human monocyte-derived dendritic cells. *Proc Natl Acad Sci* **106**: 2735–2740. doi:10.1073/pnas.0811073106
- Chen KR, Yu CK, Kung SH, Chen SH, Chang CF, Ho TC, Lee YP, Chang HC, Huang LY, Lo SY, et al. 2018. Toll-like receptor 3 is involved in detection of enterovirus A71 infection and targeted by viral 2A protease. *Viruses* **10**: E689. doi:10.3390/v10120689
- Fukushima Y, Okamoto M, Ishikawa K, Kouwaki T, Tsukamoto H, Oshiumi H. 2018. Activation of TLR3 and its adaptor TICAM-1 increases miR-21 levels in extracellular vesicles released from human cells. *Biochem Biophys Res Commun* **500**: 744–750. doi:10.1016/j.bbrc.2018.04.146
- Garmaroudi FS, Marchant D, Hendry R, Luo H, Yang D, Ye X, Shi J, McManus BM. 2015. Coxsackievirus B3 replication and pathogenesis. *Future Microbiol* **10**: 629–653. doi:10.2217/fmb.15.5
- Ghose J, Sinha M, Das E, Jana NR, Bhattacharyya NP. 2011. Regulation of miR-146a by RelA/NFκB and p53 in STHdhQ111/HdhQ111 cells, a cell model of Huntington's disease. *PLoS One* **6**: e23837. doi:10.1371/journal.pone.0023837
- Gui J, Yue Y, Chen R, Xu W, Xiong S. 2012. A20 (TNFAIP3) alleviates CVB3-induced myocarditis via inhibiting NF-κB signaling. *PLoS One* **7**: e46515. doi:10.1371/journal.pone.0046515
- He X, Jing Z, Cheng G. 2014. MicroRNAs: new regulators of Toll-like receptor signaling pathways. *Biomed Res Int* **2014**: 1–14.
- Ho BC, Yu IS, Lu LF, Rudensky A, Chen HY, Tsai CW, Chang YL, Wu CT, Chang LY, Shih SR, et al. 2015. Inhibition of miR-146a prevents enterovirus-induced death by restoring the production of type I interferon. *Nat Commun* **5**: 3344.
- Janssens S, Beyaert R. 2003. Role of Toll-like receptors in pathogen recognition. *Clin Microbiol Rev* **16**: 637–646. doi:10.1128/CMR.16.4.637-646.2003
- Jiang C, Zhu W, Xu J, Wang B, Hou W, Zhang R, Zhong N, Ning Q, Han Y, Yu H, et al. 2014. MicroRNA-26a negatively regulates Toll-like receptor 3 expression of rat macrophages and ameliorates pristane induced arthritis in rats. *Arthritis Res Ther* **16**: R9. doi:10.1186/ar4435

- Johnnidis JB, Harris MH, Wheeler RT, Stehling-Sun S, Lam MH, Kirak O, Brummelkamp TR, Fleming MD, Camargo FD. 2008. Regulation of progenitor cell proliferation and granulocyte function by microRNA-223. *Nature* **451**: 1125–1129. doi:10.1038/nature06607
- Kamali K, Korjan ES, Eftekhari E, Malekzadeh K, Soufi FG. 2016. The role of miR-146a on NF- κ B expression level in human umbilical vein endothelial cells under hyperglycemic condition. *Bratisl Med J* **117**: 376–380. doi:10.4149/BLL_2016_074
- Kawai T, Akira S. 2007. Signaling to NF- κ B by Toll-like receptors. *Trends Mol Med* **13**: 460–469. doi:10.1016/j.molmed.2007.09.002
- Kawai T, Akira S. 2011. Toll-like receptors and their crosstalk with other innate receptors in infection and immunity. *Immunity* **34**: 637–650. doi:10.1016/j.immuni.2011.05.006
- Kim K-S, Chapman NM, Tracy S. 2008. Replication of coxsackievirus B3 in primary cell cultures generates novel viral genome deletions. *J Virol* **82**: 2033–2037. doi:10.1128/JVI.01774-07
- Labbaye C, Testa U. 2012. The emerging role of MIR-146A in the control of hematopoiesis, immune function and cancer. *J Hematol Oncol* **5**: 13. doi:10.1186/1756-8722-5-13
- Lee H-M, Kim TS, Jo E-K. 2016. MiR-146 and miR-125 in the regulation of innate immunity and inflammation. *BMB Rep* **49**: 311–318. doi:10.5483/BMBRep.2016.49.6.056
- Li Y-L, Wang J, Zhang C-Y, Shen Y-Q, Wang H-M, Ding L, Gu Y-C, Lou J-T, Zhao X-T, Ma Z-L, et al. 2016. MiR-146a-5p inhibits cell proliferation and cell cycle progression in NSCLC cell lines by targeting CCND1 and CCND2. *Oncotarget* **7**: 59287–59298.
- Livak KJ, Schmittgen TD. 2001. Analysis of relative gene expression data using real-time quantitative PCR and the $2^{-\Delta\Delta CT}$ method. *Methods* **25**: 402–408. doi:10.1006/meth.2001.1262
- Marchant D, Si X, Luo H, McManus B, Yang D. 2008. The impact of CVB3 infection on host cell biology. *Curr Top Microbiol Immunol* **323**: 177–198. doi:10.1007/978-3-540-75546-3_8
- Matsumoto M, Oshiumi H, Seya T. 2011. Antiviral responses induced by the TLR3 pathway. *Rev Med Virol* **21**: 67–77. doi:10.1002/rmv.680
- Min SK, Kim MJ, Jung SY, Kang HK, Bin JS, Min BM. 2017. MicroRNA-146a-5p limits elevated TGF- β signal during cell senescence. *Mol Ther Nucleic Acids* **7**: 335–338. doi:10.1016/j.omtn.2017.04.016
- O'Neill LA, Sheedy FJ, McCoy CE. 2011. MicroRNAs: the fine-tuners of Toll-like receptor signaling. *Nat Rev Immunol* **268**: 262–268.
- Oshiumi H, Okamoto M, Fujii K, Kawanishi T, Matsumoto M, Koike S, Seya T. 2011. The TLR3/TICAM-1 pathway is mandatory for innate immune responses to poliovirus infection. *J Immunol* **187**: 5320–5327. doi:10.4049/jimmunol.1101503
- Pérez De Diego R, Mulvey C, Casanova JL, Godovac-Zimmermann J. 2014. Proteomics in immunity and herpes simplex encephalitis. *Expert Rev Proteomics* **11**: 21–29. doi:10.1586/14789450.2014.864954
- Sanghavi SK, Reinhart TA. 2014. Increased expression of TLR3 in lymph nodes during simian immunodeficiency virus infection: implications for inflammation and immunodeficiency. *J Immunol* **175**: 5314–5323. doi:10.4049/jimmunol.175.8.5314
- Sesti-Costa R, Françoço MCS, Silva GK, Proenca-Modena JL, Silva JS. 2017. TLR3 is required for survival following Coxsackievirus B3 infection by driving T lymphocyte activation and polarization: the role of dendritic cells. *PLoS One* **12**: e0185819. doi:10.1371/journal.pone.0185819
- Taganov KD, Boldin MP, Chang K-J, Baltimore D. 2006. NF- κ B-dependent induction of microRNA miR-146, an inhibitor targeted to signaling proteins of innate immune responses. *Proc Natl Acad Sci* **103**: 12481–12486. doi:10.1073/pnas.0605298103
- Tatematsu M, Nishikawa F, Seya T, Matsumoto M. 2013. Toll-like receptor 3 recognizes incomplete stem structures in single-stranded viral RNA. *Nat Commun* **4**: 1833. doi:10.1038/ncomms2857
- Tili E, Michaille J-J, Cimino A, Costinean S, Dumitru CD, Adair B, Fabbri M, Alder H, Liu CG, Calin GA, et al. 2007. Modulation of miR-155 and miR-125b levels following lipopolysaccharide/TNF- α stimulation and their possible roles in regulating the response to endotoxin shock. *J Immunol* **179**: 5082–5089. doi:10.4049/jimmunol.179.8.5082
- Tong L, Lin L, Zhao W, Wang B, Wu S, Liu H, Zhong X, Cui Y, Gu H, Zhang F, et al. 2011. Destabilization of coxsackievirus B3 genome integrated with enhanced green fluorescent protein gene. *Intervirology* **54**: 268–275. doi:10.1159/000321351
- Tong L, Lin L, Wu S, Guo Z, Wang T, Qin Y, Wang R, Zhong X, Wu X, Wang Y, et al. 2013. MiR-10a* up-regulates coxsackievirus B3 biosynthesis by targeting the 3D-coding sequence. *Nucleic Acids Res* **41**: 3760–3771. doi:10.1093/nar/gkt058
- Trobaugh DW, Klimstra WB. 2017. MicroRNA regulation of RNA virus replication and pathogenesis. *Trends Mol Med* **23**: 80–93. doi:10.1016/j.molmed.2016.11.003
- Verma B, Bhattacharyya S, Das S. 2010. Polypyrimidine tract-binding protein interacts with coxsackievirus B3 RNA and influences its translation. *J Gen Virol* **91**: 1245–1255. doi:10.1099/vir.0.018507-0
- Wang L, Qin Y, Tong L, Wu S, Wang Q, Jiao Q, Guo Z, Lin L, Wang R, Zhao W, et al. 2012. MiR-342-5p suppresses coxsackievirus B3 biosynthesis by targeting the 2C-coding region. *Antiviral Res* **93**: 270–279. doi:10.1016/j.antiviral.2011.12.004
- Wang M, Gao Z, Pan L, Zhang Y. 2014. Cellular microRNAs and picornaviral infections. *RNA Biol* **11**: 808–816. doi:10.4161/rna.29357
- Wu X, Wu S, Tong L, Luan T, Lin L, Lu S, Zhao W, Ma Q, Liu H, Zhong Z. 2009. miR-122 affects the viability and apoptosis of hepatocellular carcinoma cells. *Scand J Gastroenterol* **44**: 1332–1339. doi:10.3109/00365520903215305
- Wu J, Shen L, Chen J, Xu H, Mao L. 2015. The role of microRNAs in enteroviral infections. *Brazilian J Infect Dis* **19**: 510–516. doi:10.1016/j.bjid.2015.06.011
- Ye X, Hemida MG, Qiu Y, Hanson PJ, Zhang HM, Yang D. 2013. MiR-126 promotes coxsackievirus replication by mediating cross-talk of ERK1/2 and Wnt/ β -catenin signal pathways. *Cell Mol Life Sci* **70**: 4631–4644. doi:10.1007/s00018-013-1411-4
- Yin D, Li J, Lei X, Liu Y, Yang Z, Chen K. 2014. Antiviral activity of total flavonoid extracts from *Selaginella moellendorffii* hieron against coxsackie virus B3 *in vitro* and *in vivo*. *Evid Based Complement Alternat Med* **2014**: 950817.
- Zhang Q, Xiao Z, He F, Zou J, Wu S, Liu Z. 2013. MicroRNAs regulate the pathogenesis of CVB3-induced viral myocarditis. *Intervirology* **56**: 104–113. doi:10.1159/000343750
- Zheng W, Shi H, Chen Y, Xu Z, Chen J, Jin L. 2017. Alteration of serum high-mobility group protein 1 (HMGB1) levels in children with enterovirus 71-induced hand, foot, and mouth disease. *Medicine (Baltimore)* **96**: e6764. doi:10.1097/MD.0000000000006764